# Thin-Film Composite Polyamide Membranes Functionalized with Biocidal Graphene Oxide Nanosheets

François Perreault, Marissa E. Tousley, and Menachem Elimelech*

Department of Chemical and Environmental Engineering, Yale University, New Haven, Connecticut 06520-8286, United States

Ⓢ *Supporting Information*

ABSTRACT: Fouling of membranes by microorganisms is a major limiting factor in membrane separation processes. Novel strategies are therefore required to decrease the extent of bacterial growth on membranes. In this study, we confer strong antimicrobial properties to thin-film composite polyamide membranes by a simple graphene oxide surface functionalization. Using amide coupling between carboxyl groups of graphene oxide and carboxyl groups of the polyamide active layer, graphene oxide is irreversibly bound to the membrane. Surface binding of graphene oxide is demonstrated by scanning electron microscopy and Raman spectroscopy. Direct contact

of bacteria with functionalized graphene oxide on the membrane surface results in 65% bacterial inactivation after 1 h of contact time. This bactericidal effect is imparted to the membrane without any detrimental effect to the intrinsic membrane transport properties. Our results suggest that functionalization of thin-film composite membranes with graphene oxide nanosheets is a promising approach for the development of novel antimicrobial membranes.
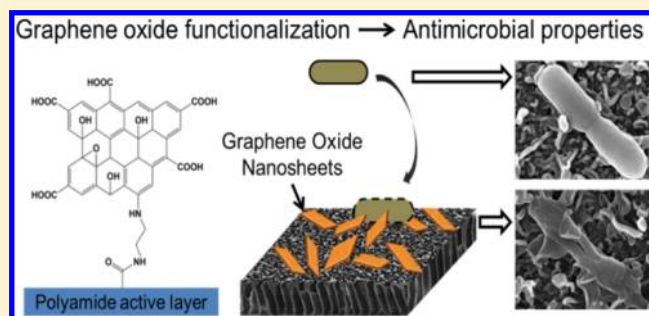
■ INTRODUCTION

Biofouling, the growth of microorganisms into a biofilm, is a major limiting factor in membrane separation processes,[1] resulting in a decrease in permeate water flux and membrane selectivity, an increase in energy consumption, and a decrease in the extent of membrane survival.[2] While pretreatment of a feed effluent can reduce the number of microorganisms reaching the membrane, it cannot completely remove all bacterial cells, which colonize and multiply on the membrane surface to form biofilms. Thin-film composite (TFC) polyamide membranes, the most widely used type of membranes for reverse osmosis, engineered osmosis, and nanofiltration, are particularly susceptible to biofouling. Because these membranes are sensitive to degradation by common disinfectants, such as chlorine, novel strategies for controlling biofilm development are needed.[1]

Modification of TFC membranes with antimicrobial nano-materials is a promising approach to increasing antimicrobial activity and therefore biofouling resistance.[3,4] The antimicrobial efficiency of biocide-releasing nanomaterials attached to the membrane surface, such as silver nanoparticles, has already been demonstrated.[5,6] Biocide release, however, leads to a loss of antimicrobial activity over time. In addition, the release of biocides to the environment can be problematic for large-scale application. Alternatively, carbon-based nanomaterials, such as carbon nanotubes and graphene, may be promising for membrane modification, as they have been shown to inactivate bacteria upon contact with bacterial cells.[7−11] This bactericidal effect does not become weaker over time, allowing for a new type of nonleaching, nondepleting antimicrobial surface.

Previous work on TFC membrane functionalization with single-walled carbon nanotubes (SWNTs) demonstrates the effectiveness of this strategy in conferring antimicrobial activity.[12]

Graphene, consisting of single-atom-thick sheets of sp²-bonded carbon, has attracted an increasing level of attention for a new generation of applications based on carbon nanomaterials.[13] Interest in this material in membrane development is rooted in its inherent smoothness, atomic-level thickness, and high water slip length.[14,15] Furthermore, graphene's oxidized form, graphene oxide, can be produced at relatively low cost through chemical oxidation of graphite.[16,17]

Several studies have focused on incorporating graphene oxide into polymer casting solutions used during membrane fabrication for antimicrobial properties, increased permeability, and enhanced mechanical strength.[18−21] While this approach has yielded performance enhancements, the majority of the graphene oxide was embedded in the bulk of the membrane, rendering it unavailable for surface-based interactions. The antimicrobial effect of graphene oxide nanosheets, for example, is significantly enhanced by direct contact with the bacterial cells.[8,11] Thus, postfabrication surface functionalization will allow the concentration of graphene oxide nanosheets at the membrane surface, rendering them readily available for inactivation of bacteria. Additionally, surface functionalization
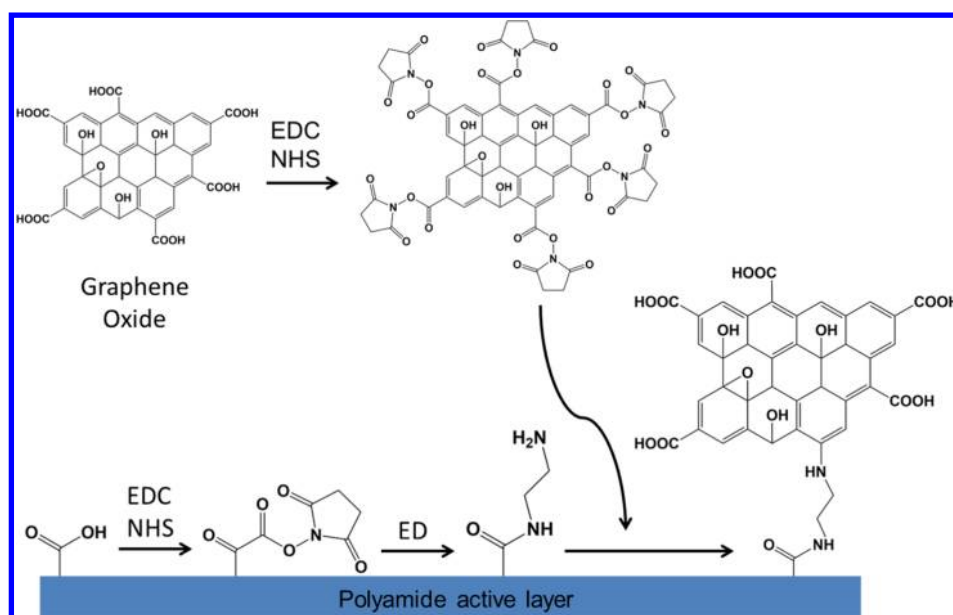
Figure 1. Reaction scheme for covalent binding of graphene oxide to the active layer of thin-film composite (TFC) polyamide membranes. Native carboxyl groups of the polyamide active layer and of the graphene oxide sheets are first converted to amine-reactive esters with 1-ethyl-3-[3-(dimethylamino)propyl]carbodiimide (EDC) and N-hydroxysuccinimide (NHS) and then bound together using an ethylenediamine (ED) cross-linker.

substantially reduces the amount of nanomaterial required for the modification, and hence the cost and associated environmental impacts of graphene oxide manufacturing. To date, however, no studies have functionalized membranes with graphene oxide via surface modification to improve membrane antimicrobial activity.

In this study, we present the first demonstration of surface functionalization of TFC polyamide membranes with graphene oxide for the introduction of antimicrobial properties. Graphene oxide nanosheets were covalently bound to the polyamide active layer of the membrane, allowing efficient bacterial cell inactivation without altering the intrinsic water and salt permeabilities. Our results highlight the potential of graphene oxide in the design of new antimicrobial TFC membranes. In addition, the simple functionalization procedure allows further development of graphene oxide as a membrane modification platform for a wide range of applications.

MATERIALS AND METHODS

Synthesis and Characterization of Graphene Oxide. Graphite was chemically exfoliated to produce graphene oxide, adapting a method described by Marcano et al.[22] The oxidized sp^2 graphitic structure was confirmed by Raman spectroscopy (Figure S1A of the Supporting Information). The different oxygen-containing groups present in graphene oxide were identified by X-ray photoelectron spectroscopy (XPS) (Figure S1B of the Supporting Information). The size and thickness of graphene oxide sheets were evaluated by atomic force microscopy (AFM) (Figure S1C,D of the Supporting Information). Detailed procedures and data are given in the Supporting Information.

Thin-Film Composite Membrane Fabrication. TFC membranes were prepared by interfacial polymerization of polyamide onto a hand-cast polysulfone support layer, as described in a previous publication.[23] Polysulfone support layers were fabricated on a nonwoven commercial polyester fabric by phase inversion, using a 12% polysulfone solution in

N-methyl-2-pyrrolidone. Polysulfone was spread on the polyester fabric using a casting knife with a gate height of ~250 μm (10 mils). The polyamide active layer was then polymerized by immersing an m-phenylenediamine-saturated polysulfone support layer into a trimesoyl chloride solution in Isopar-G. Details of the TFC membrane fabrication are given in the Supporting Information.

Membrane Functionalization and Characterization. TFC membranes were functionalized with graphene oxide using 1-ethyl-3-[3-(dimethylamino)propyl]carbodiimide hydrochloride (EDC)- and N-hydroxysuccinimide (NHS)-mediated activation of carboxyl groups (Figure 1). The polyamide carboxyl groups were first converted into amine-reactive esters by contacting the membrane with EDC and NHS. Ethylenediamine (ED) was then attached to the membrane active layer by the formation of amide bonds with the activated esters. The free amine groups of ED were used to bind EDC- and NHS-activated graphene oxide to the active layer of the TFC membrane.

Binding of graphene oxide to TFC membranes was verified by scanning electron microscopy (SEM) and Raman spectroscopy. Raman mapping was used to quantify the coverage of graphene oxide on the membrane. The intrinsic transport properties (pure water permeability, A, and salt permeability, B) and salt (NaCl) rejection, R, of the membranes were determined in a laboratory-scale crossflow reverse osmosis unit at an operating pressure of 27.6 bar (400 psi) and a crossflow velocity of 21.4 cm s^{-1}. For the measurement of R, a feed solution of 50 mM NaCl was used. Additional details about functionalization and characterization are provided in the Supporting Information.

Antimicrobial Activity of Graphene Oxide-Functionalized Membranes. Bacterial inactivation was evaluated by a plate counting method as described in the Supporting Information. Briefly, an *Escherichia coli* K12 suspension (10^7 colony-forming units/mL) was contacted with the membrane surface (0.5 mL/cm^2) for 1 h at room temperature. Then, the
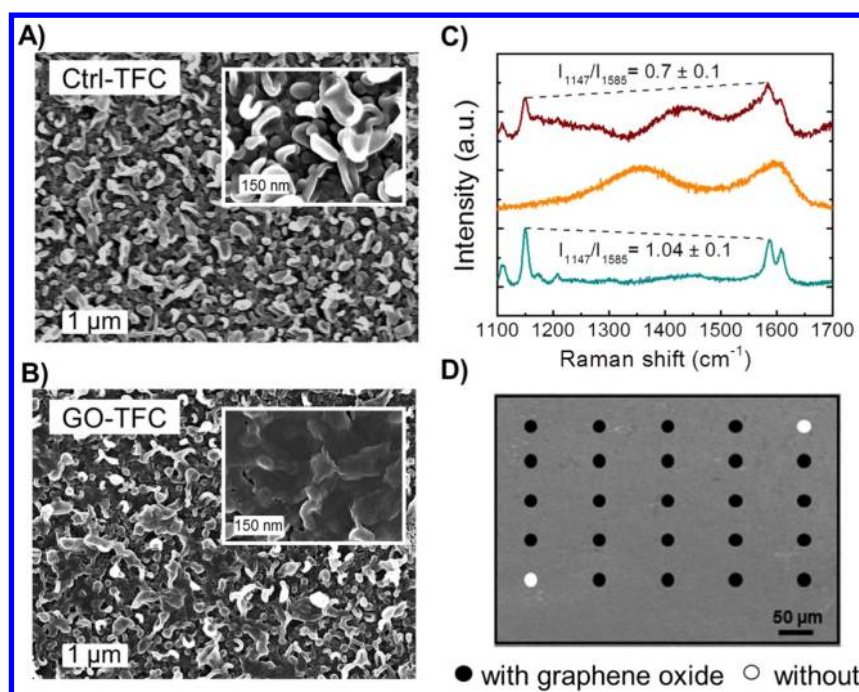
Figure 2. Characterization of the control (Ctrl-TFC) and graphene oxide-functionalized (GO-TFC) membranes. (A) Representative SEM micrograph of the polyamide active layer of the Ctrl-TFC membrane. (B) Representative SEM micrograph of the polyamide active layer of the GO-TFC membrane. (C) Raman spectra of Ctrl-TFC (blue), graphene oxide (orange), and GO-TFC (brown). The ratio between the peaks at 1147 and 1585 cm^{-1} was used as an indicator of the presence of GO on the polyamide active layer. (D) Representative Raman mapping image of GO-TFC. The dots indicate the different measurement points on the membrane surface. The presence of graphene oxide (black dots) was identified by an I_{1147}/I_{1585} ratio that was significantly lower than the average Ctrl-TFC value (95% confidence interval).

suspension was removed, and the membrane coupons were washed thoroughly with a 0.9% sterile saline solution. The membrane coupons were bath sonicated for 7 min to remove the bacteria from the membrane surface. Bacteria were spread on agar plates and incubated overnight at 37 °C. Additionally, bacteria were fixed and sputter-coated with chromium for SEM imaging, as described in the Supporting Information.

■ RESULTS AND DISCUSSION

Graphene Oxide Binds Irreversibly to the Membrane Surface. AFM imaging reveals that our graphene oxide synthesis produced nanosheets of one (∼1.7 nm thick) to a few layers of carbon atoms (Figure S1C,D of the Supporting Information), with lateral sizes ranging from 30 to 650 nm, as determined by SEM image analysis (data not shown). XPS analysis indicates that ∼69% of carbon atoms were oxidized to C═O, C−OH, or −COOH bonds (Figure S1B of the Supporting Information). The carboxyl groups of graphene oxide were used for covalent binding to the TFC active layer via EDC- and NHS-mediated amide coupling,[17,24] as described in Figure 1. The polyamide layer was first reacted with EDC and NHS to bind ED to the native carboxyl groups of the active layer, increasing the number of amine groups available at the membrane surface (Figure 1). Graphene oxide nanosheets were also reacted with EDC and NHS to activate the carboxyl groups and then contacted with the amine-rich membrane surface for covalent binding. Graphene oxide-functionalized TFC (GO-TFC) membranes were then bath sonicated to remove loosely bound nanosheets. SEM micrographs of GO-TFC membranes reveal the presence of graphene oxide nanosheets irreversibly bound to the polyamide layer after sonication (Figure 2B).

The binding of graphene oxide to TFC membranes was further demonstrated by Raman spectroscopy. The Raman spectrum of the Ctrl-TFC membrane is mainly characterized by the signal of its thick polysulfone layer, with the two dominant peaks originating from the symmetric C−O−C stretching (1147 cm^{-1}) and phenyl ring vibration (1585 cm^{-1}) of polysulfone (Figure 2C).[25,26] Graphene oxide, on the other hand, has two characteristic broad peaks at 1350 (D band) and 1590 cm^{-1} (G band). In graphene oxide-functionalized membranes, the presence of graphene oxide results in peak broadening at 1585 cm^{-1} due to combined contributions from the polysulfone phenyl ring vibration and the graphene G band. For the same reason, graphene oxide incorporation also induces a change in the polysulfone C−O−C stretching and phenyl ring vibration band ratio (I_{1147}/I_{1585}). The I_{1147}/I_{1585} ratio significantly decreased from 1.04 in Ctrl-TFC membranes to 0.7 in GO-TFC membranes ($p = 0.0004$), confirming the binding of graphene oxide to the TFC membrane. The I_{1147}/I_{1585} ratio was also used to evaluate the coverage of the membrane by graphene oxide using Raman mapping. From 25 individual spectra taken on a 200 μm × 250 μm grid, an average of 78.6% of the GO-TFC surface showed an I_{1147}/I_{1585} smaller than the 95% confidence interval range of the Ctrl-TFC I_{1147}/I_{1585} ratio, indicating the presence of graphene oxide on the membrane surface (Figure 2D). Our functionalization protocol was thus successful in providing good coverage of the TFC membrane with graphene oxide nanosheets.

Membrane Transport Properties Are Not Impacted by Graphene Oxide Functionalization. Intrinsic membrane transport properties were evaluated to determine how graphene oxide functionalization impacted the performance of the membrane. The pure water permeability coefficient, *A*, and the salt permeability coefficient, *B*, of the GO-TFC membrane
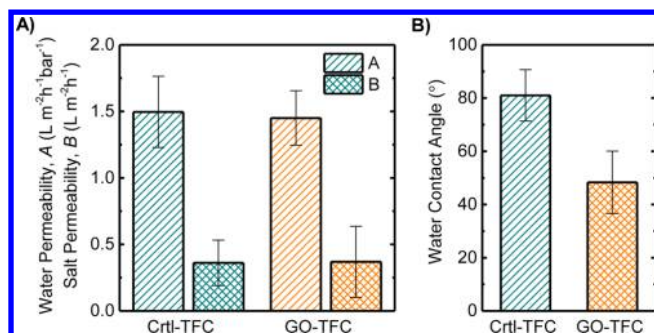
Figure 3. Membrane properties of Ctrl-TFC and GO-TFC membranes. (A) Water permeability coefficient, A, and salt (NaCl) permeability coefficient, B, of Ctrl-TFC and GO-TFC membranes. (B) Water contact angle for Ctrl-TFC and GO-TFC membranes.

Figure 4. (A) Colony-forming units after *E. coli* cells had been in contact with the membranes for 1 h at room temperature. (B) SEM micrograph showing normal *E. coli* cells at the surface of the Ctrl-TFC membrane. (C and D) SEM micrographs showing compromised *E. coli* cells at the surface of the GO-TFC membrane active layer. Compromised cells are denoted with an arrow in panel C.

were not significantly different than those of the Ctrl-TFC membrane ($p > 0.05$) (Figure 3A). Salt rejection values of 98.2 ± 1.2 and 97.8 ± 0.8% were obtained for the Ctrl-TFC and GO-TFC membranes, respectively. Therefore, functionalization of the active layer with graphene oxide nanosheets did not have any deleterious effect on membrane performance. This observation represents a significant advance as surface modifications of TFC membranes often result in a concomitant decrease in water permeability and selectivity.[27−29]

Membrane surface hydrophilicity was evaluated by measuring the water contact angle. Pristine TFC membranes were relatively hydrophobic with a contact angle of 81°. Graphene oxide functionalization significantly increased the hydrophilicity of the membrane, decreasing the water contact angle to 47° (Figure 3B). This observation is attributed to the oxygen-containing functional groups of graphene oxide, as discussed earlier. In marked contrast to our graphene oxide surface functionalization, the maximal decrease in contact angle observed for graphene oxide-blended PVDF membranes was from 79.2° to 60.7°, at a relatively high concentration (0.2 wt %) of graphene oxide.[30] Consequently, surface functionalization, during which nanosheets are concentrated at the surface, has a stronger effect on the membrane hydrophilicity, which allows for finer tuning of membrane properties. We note that the change in surface hydrophilicity does not affect membrane water permeability as the transport of water is governed by a solution−diffusion mechanism through the polyamide active layer,[1] which was not impacted by our surface functionalization.

The Functionalized Membrane Exhibits Strong Antimicrobial Activity. Graphene oxide functionalization imparted strong antimicrobial activity to the membrane, reducing the number of viable *E. coli* cells by 64.5% after contact with the membrane for 1 h (Figure 4A). Recent studies have proposed that, like the SWNT inactivation mechanism,[31,32] graphene oxide inactivates bacteria upon direct cell contact by inducing membrane damage, mediated by physical disruption,[7] charge transfer and formation of reactive oxygen species,[7,8] and extraction of lipid from the cell membrane.[11] SEM imaging of bacterial cells attached to the membrane surface confirmed cell damage induced by the graphene oxide-functionalized membrane. Most cells attached to the GO-TFC membrane exhibit compromised integrity and appear to be flattened or shrunk (Figure 4C,D and Figure S3 of the Supporting Information) compared to cells attached to the Ctrl-TFC membrane (Figure 4B).
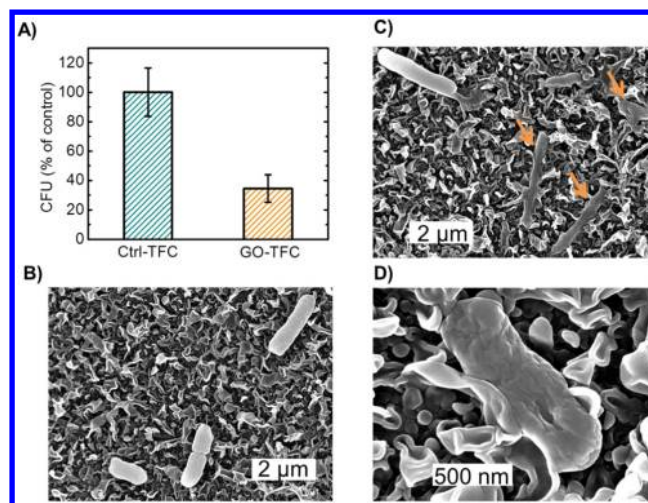
In comparison, for the same contact time (1 h), the extent of *E. coli* inactivation was found to be 59% for graphene oxide nanowalls electrodeposited on stainless steel[7] and 42% for indium−tin oxide coated with a polymer−graphene oxide nanocomposite.[33] Therefore, graphene oxide-functionalized membranes effectively decreased the number of attached viable cells despite the thin, nonvisible graphene oxide coating on the membrane surface (Figure S2 of the Supporting Information). Inactivation of bacteria by graphene oxide-coated surfaces is also dependent on contact time with the bacterial cells, with higher inactivation rates reported for higher contact times.[33,34]

Graphene oxide surface functionalization was effective in providing a strong antimicrobial activity, comparable to that of other membranes functionalized with carbon nanomaterials.[12,19] However, the higher hydrophilicity of the resulting membrane and the low cost of graphene oxide production render this approach promising for the future development of antimicrobial membranes based on carbon nanomaterials. Because of the requirement for close contact between nanosheets and bacterial cells, future improvement may be possible by optimizing the membrane coverage by graphene oxide. In addition, fine-tuning the oxygen content and sheet dimensions of graphene oxide, which were shown to influence oxidizing potential and antibacterial activity,[7,8,35,36] may also enhance the antimicrobial effect of graphene oxide-functionalized membranes.

■ ASSOCIATED CONTENT

Ⓢ Supporting Information

Complete materials and methods information; Raman spectroscopy, XPS spectroscopy, and AFM imaging of graphene oxide nanosheets (Figure S1); images of the Ctrl-TFC and GO-TFC membranes (Figure S2); and additional SEM images of bacterial cells on GO-TFC membranes (Figure S3). This material is available free of charge via the Internet at http://pubs.acs.org.

■ AUTHOR INFORMATION

Corresponding Author
*E-mail: menachem.elimelech@yale.edu. Phone: (203) 432-2789.

Notes
The authors declare no competing financial interest.

■ REFERENCES

(1) Elimelech, M.; Phillip, W. A. The Future of Seawater Desalination: Energy, Technology, and the Environment. *Science* **2011**, *333*, 712−717.

(2) Matin, A.; Khan, Z.; Zaidi, S. M. J.; Boyce, M. C. Biofouling in Reverse Osmosis Membranes for Seawater Desalination: Phenomena and Prevention. *Desalination* **2011**, *281*, 1−16.

(3) Li, Q.; Mahendra, S.; Lyon, D. Y.; Brunet, L.; Liga, M. V.; Li, D.; Alvarez, P. J. J. Antimicrobial Nanomaterials for Water Disinfection and Microbial Control: Potential Applications and Implications. *Water Res.* **2008**, *42*, 4591−4602.

(4) Banerjee, I.; Pangule, R. C.; Kane, R. S. Antifouling Coatings: Recent Developments in the Design of Surfaces That Prevent Fouling by Proteins, Bacteria, and Marine Organisms. *Adv. Mater.* **2011**, *23*, 690−718.

(5) Yin, J.; Yang, Y.; Hu, Z.; Deng, B. Attachment of Silver Nanoparticles (AgNPs) onto Thin-Film Composite (TFC) Membranes through Covalent Bonding to Reduce Membrane Biofouling. *J. Membr. Sci.* **2013**, *441*, 73−82.

(6) Lee, S. Y.; Kim, H. J.; Patel, R.; Im, S. J.; Kim, J. H.; Min, B. R. Silver Nanoparticles Immobilized on Thin Film Composite Polyamide Membrane: Characterization, Nanofiltration, Antifouling Properties. *Polym. Adv. Technol.* **2007**, *18*, 562−568.

(7) Akhavan, O.; Ghaderi, E. Toxicity of Graphene and Graphene Oxide Nanowalls Against Bacteria. *ACS Nano* **2010**, *4*, 5731−5736.

(8) Liu, S.; Zeng, T. H.; Hofmann, M.; Burcombe, E.; Wei, J.; Jiang, R.; Kong, J.; Chen, Y. Antibacterial Activity of Graphite, Graphite Oxide, Graphene Oxide, and Reduced Graphene Oxide: Membrane and Oxidative Stress. *ACS Nano* **2011**, *5*, 6971−6980.

(9) Vecitis, C. D.; Zodrow, K. R.; Kang, S.; Elimelech, M. Electronic-Structure-Dependent Bacterial Cytotoxicity of Single-Walled Carbon Nanotubes. *ACS Nano* **2010**, *4*, 5471−5479.

(10) Kang, S.; Pinault, M.; Pfefferle, L. D.; Elimelech, M. Single-Walled Carbon Nanotubes Exhibit Strong Antimicrobial Activity. *Langmuir* **2007**, *23*, 8670−8673.

(11) Tu, Y.; Lv, M.; Xiu, P.; Huynh, T.; Zhang, M.; Castelli, M.; Liu, Z.; Huang, Q.; Fan, C.; Fang, H.; Zhou, R. Destructive Extraction of Phospholipids from *Escherichia coli* Membranes by Graphene Nanosheets. *Nat. Nanotechnol.* **2013**, *8*, 594−601.

(12) Tiraferri, A.; Vecitis, C. D.; Elimelech, M. Covalent Binding of Single-Walled Carbon Nanotubes to Polyamide Membranes for Antimicrobial Surface Properties. *ACS Appl. Mater. Interfaces* **2011**, *3*, 2869−2877.

(13) Novoselov, K. S.; Fal'ko, V. I.; Colombo, L.; Gellert, P. R.; Schwab, M. G.; Kim, K. A Roadmap for Graphene. *Nature* **2012**, *490*, 192−200.

(14) Nair, R. R.; Wu, H. A.; Jayaram, P. N.; Grigorieva, I. V.; Geim, A. K. Unimpeded Permeation of Water through Helium-Leak-Tight Graphene-Based Membranes. *Science* **2012**, *335*, 442−444.

(15) Hu, M.; Mi, B. Enabling Graphene Oxide Nanosheets as Water Separation Membranes. *Environ. Sci. Technol.* **2013**, *47*, 3715−3723.

(16) Hummers, W. S.; Offeman, R. E. Preparation of Graphitic Oxide. *J. Am. Chem. Soc.* **1958**, *80*, 1339.

(17) Dreyer, D. R.; Park, S.; Bielawski, C. W.; Ruoff, R. S. The Chemistry of Graphene Oxide. *Chem. Soc. Rev.* **2010**, *39*, 228−240.

(18) Wang, Z.; Yu, H.; Xia, J.; Zhang, F.; Li, F.; Xia, Y.; Li, Y. Novel GO-Blended PVDF Ultrafiltration Membranes. *Desalination* **2012**, *299*, 50−54.

(19) Yu, L.; Zhang, Y.; Zhang, B.; Liu, J.; Zhang, H.; Song, C. Preparation and Characterization of HPEI-GO/PES Ultrafiltration Membrane with Antifouling and Antibacterial Properties. *J. Membr. Sci.* **2013**, *447*, 452−462.

(20) Zhang, J.; Xu, Z.; Shan, M.; Zhou, B.; Li, Y.; Li, B.; Niu, J.; Qian, X. Synergetic Effects of Oxidized Carbon Nanotubes and Graphene Oxide on Fouling Control and Anti-Fouling Mechanism of Polyvinylidene Fluoride Ultrafiltration Membranes. *J. Membr. Sci.* **2013**, *448*, 81−92.

(21) Lee, J.; Chae, H.-R.; Won, Y. J.; Lee, K.; Lee, C.-H.; Lee, H. H.; Kim, I.-C.; Lee, J. Graphene Oxide Nanoplatelets Composite Membrane with Hydrophilic and Antifouling Properties for Wastewater Treatment. *J. Membr. Sci.* **2013**, *448*, 223−230.

(22) Marcano, D. C.; Kosynkin, D. V.; Berlin, J. M.; Sinitskii, A.; Sun, Z.; Slesarev, A.; Alemany, L. B.; Lu, W.; Tour, J. M. Improved Synthesis of Graphene Oxide. *ACS Nano* **2010**, *4*, 4806−4814.

(23) Tiraferri, A.; Yip, N. Y.; Phillip, W. A.; Schiffman, J. D.; Elimelech, M. Relating Performance of Thin-Film Composite Forward Osmosis Membranes to Support Layer Formation and Structure. *J. Membr. Sci.* **2011**, *367*, 340−352.

(24) Sehgal, D.; Vijay, I. K. A Method for the High Efficiency of Water-Soluble Carbodiimide-Mediated Amidation. *Anal. Biochem.* **1994**, *218*, 87−91.

(25) Shilton, S. J.; Prokhorov, K. A.; Gordeyev, S. A.; Nikolaeva, G. Y.; Dunkin, I. R.; Smith, W. E.; Pashinin, P. P. Raman Spectroscopic Evaluation of Molecular Orientation in Polysulfone. *Laser Phys. Lett.* **2004**, *1*, 336−339.

(26) Kim, H. J.; Fouda, A. E.; Jonasson, K. In Situ Study on Kinetic Behavior During Asymmetric Membrane Formation via Phase Inversion Process Using Raman Spectroscopy. *J. Appl. Polym. Sci.* **1999**, *75*, 135−141.

(27) Wei, X.; Wang, Z.; Zhang, Z.; Wang, J.; Wang, S. Surface Modification of Commercial Aromatic Polyamide Reverse Osmosis Membranes by Graft Polymerization of 3-Allyl-5,5-Dimethylhydantoin. *J. Membr. Sci.* **2010**, *351*, 222−233.

(28) McCloskey, B. D.; Park, H. B.; Ju, H.; Rowe, B. W.; Miller, D. J.; Chun, B. J.; Kin, K.; Freeman, B. D. Influence of Polydopamine Deposition Conditions on Pure Water Flux and Foulant Adhesion Resistance of Reverse Osmosis, Ultrafiltration, and Microfiltration Membranes. *Polymer* **2010**, *51*, 3472−3485.

(29) Yang, H.-L.; Lin, J. C.-T.; Huang, C. Application of Nanosilver Surface Modification to RO Membrane and Spacer for Mitigating Biofouling in Seawater Desalination. *Water Res.* **2009**, *43*, 3777−3786.

(30) Wang, Z.; Yu, H.; Xia, J.; Zhang, F.; Li, F.; Xia, Y.; Li, Y. Novel GO-Blended PVDF Ultrafiltration Membranes. *Desalination* **2012**, *299*, 50−54.

(31) Kang, S.; Herzberg, M.; Rodrigues, D. F.; Elimelech, M. Antibacterial Effects of Carbon Nanotubes: Size Does Matter! *Langmuir* **2008**, *24*, 6409−6413.

(32) Pasquini, L. M.; Hashmi, S. M.; Sommer, T. J.; Elimelech, M.; Zimmerman, J. B. Impact of Surface Functionalization on Bacterial Cytotoxicity of Single-Walled Carbon Nanotubes. *Environ. Sci. Technol.* **2012**, *46*, 6297−6305.

(33) Mejías Carpio, I. E.; Santos, C. M.; Wei, X.; Rodrigues, D. F. Toxicity of a Polymer-Graphene Oxide Composite Against Bacterial Planktonic Cells, Biofilms, and Mammalian Cells. *Nanoscale* **2012**, *4*, 4746−4756.

(34) Santos, C. M.; Tria, M. C. R.; Vergara, R. A. M. V.; Ahmed, F.; Advincula, R. C.; Rodrigues, D. F. Antimicrobial Graphene Polymer (PVK-GO) Nanocomposite Films. *Chem. Commun.* **2011**, *47*, 8892−8894.

(35) Liu, S.; Hu, M.; Zeng, T. H.; Wu, R.; Jiang, R.; Wei, J.; Wang, L.; Kong, J.; Chen, Y. Lateral Dimension-Dependent Antibacterial Activity of Graphene Oxide Sheets. *Langmuir* **2012**, *28*, 12364−12372.

(36) Gurunathan, S.; Han, J. W.; Dayem, A. A.; Eppakayala, V.; Kim, J.-H. Oxidative Stress-Mediated Antibacterial Activity of Graphene Oxide and Reduced Graphene Oxide in *Pseudomonas aeruginosa*. *Int. J. Nanomed.* **2012**, *7*, 5901−5914.

F

dx.doi.org/10.1021/ez4001356 | *Environ. Sci. Technol. Lett.* XXXX, XXX, XXX−XXX